J Solid State Electrochem (2003) 7: 724–728
DOI 10.1007/s10008-003-0391-y

ORIGINAL PAPER

G. Vaivars · M. Furlani · B.-E. Mellander
C. G. Granqvist

Proton-conducting zirconium phosphate/poly(vinyl acetate)/glycerine gel electrolytes

Received: 27 November 2002 / Accepted: 11 April 2003 / Published online: 17 June 2003

Abstract This work reports on a proton gel electrolyte composed of zirconium phosphate (ZP) particles suspended in a poly(vinyl acetate)/glycerine matrix. The material was studied by X-ray powder diffraction, differential scanning calorimetry, impedance spectroscopy, and spectrophotometry. It had a proton conductivity of 1–0.1 mS/cm at room temperature and remained stable and transparent up to at least 110 °C; it therefore appears suitable for uses in electrochromic devices. The structure of the ZP powder and of the gel is discussed in terms of water removal from interplanar spaces by heating or exfoliation. It is suggested that an exfoliation of the layered structure of ZP by intercalation of glycerine produces a dispersion of ZP nanoparticles in the poly(vinyl acetate)/glycerine matrix.

Keywords Electrochromic device · Poly(vinyl acetate)/glycerine matrix · Proton gel electrolyte · Zirconium phosphate

Introduction

Electrochromic (EC) devices are able to sustain reversible changes of their optical properties under the action of a voltage [1, 2, 3]. Most practical applications require devices operating for 10–25 years without significant degradation. Furthermore, stability is needed up to ~100 °C. An ion-conducting electrolyte suitable for EC devices must have a conductivity of the order of 10^{-3} S/cm at room temperature, as well as chemical compatibility with regard to porous metal oxides such as tungsten oxide and nickel oxide. Gel electrolytes may be suitable candidates for practical uses as a result of their combined properties of a host structure and fine guest particles. However, water, normally a fundamental constituent of the gel, may be released and cause corrosion of the metal oxides, especially if the electrolyte contains acids. A practical strategy for making a non-aggressive electrolyte is then to prepare a gel whose constituents are chemically inert with regard to the metal oxides and which do not cause corrosion in the case of a partial phase separation.

Our present work deals with proton-conducting gels containing zirconium phosphate (ZP). This is a material of choice as a proton electrolyte for practical applications since it is chemically stable, non-corrosive, non-toxic, and inexpensive. ZP has been studied in the past with particular regard to its crystalline phase, whereas less attention has been paid to the amorphous structure. Amorphous powders crystallize easily, and this lack of stability may be a drawback for practical applications [4]. However, it was shown earlier [5] that amorphous ZP is suitable for nanocomposite preparation. ZP/Nafion [6, 7], sulfonated poly(ether ketones) incorporating nanosize ZP particles [8], layered zirconium sulfoarylphosphonate-based hybrid polymer membranes [9], and their application in fuel cells, have been studied with a view to high thermal stability and decreased methanol diffusion across the electrolyte (cross-over) [10, 11].

Below we report on a proton-conducting electrolyte composed of particles of ZP suspended in a matrix of poly(vinyl acetate) (PVA). We discuss methods for sample preparation and present data on materials characterization by use of X-ray diffraction (XRD), differential scanning calorimetry (DSC), impedance spectroscopy, and spectrophotometry.

C. G. Granqvist (✉)
Department of Materials Science, The Ångström Laboratory, Uppsala University, P.O. Box 534, SE-751 21 Uppsala, Sweden
E-mail: claes-goran.granqvist@angstrom.uu.se

G. Vaivars
Institute of Solid State Physics, University of Latvia, Kengaraga 8, 1063 Riga, Latvia

M. Furlani · B.-E. Mellander
Physics and Engineering Physics, Chalmers University of Technology and Göteborg University, SE-412 96 Gothenburg, Sweden

Experimental

Sample preparation

Figure 1 illustrates the synthesis procedures used in this work. An aqueous suspension of amorphous ZP, i.e. $Zr(HPO_4)_2{\cdot}nH_2O$, was produced as described by Clearfield and Stynes [12]. Powders with n being 3.7 and 2.9 were obtained by drying for 24 h under normal ambient conditions and at 160 °C, respectively. The water contents were determined by thermogravimetry, using a single-furnace Perkin-Elmer TGS-2 instrument. All of the powders were ground in an agate mortar and were then investigated by XRD.

Powders with an initial n equal to 3.7 were examined by DSC in their as-prepared state, after post treatment by drying for 24 h at 105 °C, and after a subsequent drying for 6 h under vacuum (specifically at 10^{-5} Pa).

Electrolytes were prepared by mixing an aqueous suspension of ZP with glycerine and PVA, the concentration of ZP being between 5 wt% and 30 wt%. After initial drying, the ensuing viscous slurry was transformed either to a white elastic solid by fast drying at low pressure in the presence of P_2O_5, or to a viscous transparent gel by slow drying under normal conditions. All of these materials were stable during a few years of storage under ambient conditions. The stability of the materials was monitored through measurements of the proton conductivity by impedance spectroscopy. This conductivity was found to remain constant, to within experimental accuracy, over at least four years. Furthermore, XRD measurements did not indicate any structural changes during this time span.

Results and discussion

Composition and structure

Crystallinity by XRD

XRD data were recorded on a DRON-2 diffractometer employing Co K_α radiation. Figure 2 displays a set of diffractograms. Curves (a) and (b) refer to ZP powders with n values of 3.7 and 2.9, respectively. The former of these samples displays clear peaks for diffraction angles 2θ of 12° and 34°, as well as a broad feature at $20° < 2\theta < 28°$. Heating and dehydration makes the distinct peak at $2\theta = 12°$ disappear, as apparent from curve (b). The diffractograms represented by curves (a) and (b) are consistent with α-$Zr(HPO_4)_2{\cdot}H_2O$ [13, 14], i.e. with a structure that is well known to comprise parallel layers separated by 0.76 nm [15] and held together solely by weak van der Waals forces. Specifically, the interlayer separation can be reconciled with the strong XRD peak at $2\theta = 12°$. It is evident from our data that dehydration leads to a disintegration of the layer structure. Curves (c) and (d) in Fig. 2 pertain to ZP/PVA/glycerine gels subjected to fast and slow drying, respectively. Fast drying is seen to yield a structure characterized by broad, though well developed, XRD features at $10° < 2\theta < 16°$ and $20° < 2\theta < 28°$, in addition to a peak at $2\theta = 34°$, all being consistent with the α-$Zr(HPO_4)_2{\cdot}H_2O$ structure. The broadening of the XRD features is attributed to relaxation of the crystalline parameters. Slow drying, on the other hand, produced a material with low order and a sole XRD feature at $10 < 2\theta < 12°$.

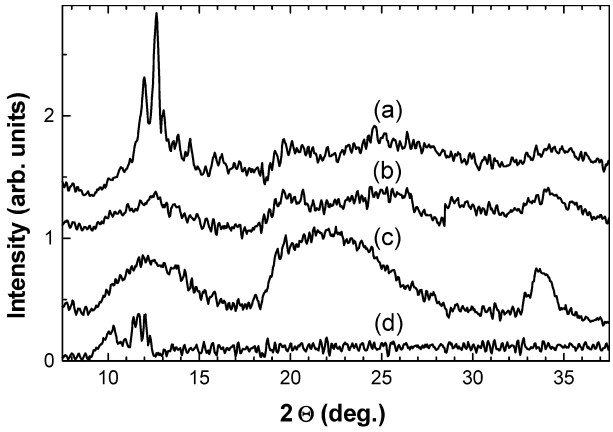

Fig. 2 XRD patterns of (*a*) $Zr(HPO_4)_2{\cdot}3.7H_2O$, (*b*) $Zr(HPO_4)_2{\cdot}2.9H_2O$, and ZP/PVA/glycerine gels after (*c*) fast and (*d*) slow drying

Figure 2 illustrates that dehydration as well as gel formation can lead to at least a partial collapse of the layer configuration of ZP. To shed some further light on this phenomenon, we note that hydrate water in ZP is accommodated in zeolitic-type cavities [15]. This water can help to maintain the three-dimensional structure, as evidenced from observations [16] that dehydration tends to decrease the interlayer spacing. Furthermore, it has been found [17] that fast removal of absorbed water during heating of large ZP crystals leads to structural disintegration. The precise degradation mode is not known for our material, but the layer structure of ZP makes us believe that exfoliation takes place so that the initial three-dimensional structure is broken up.

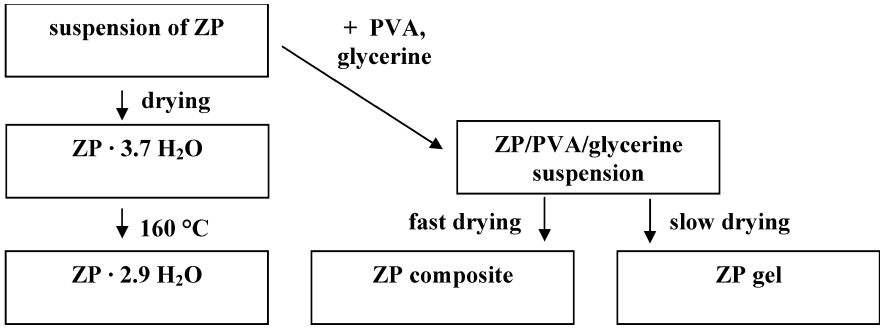

Fig. 1 Synthesis procedures of zirconium phosphate (ZP)-based proton-conducting materials. PVA denotes poly(vinyl acetate)

Regarding the structural effects of gel formation, we note that earlier work [18, 19] has demonstrated that ZP can intercalate guest molecules, which are then able to change the properties of the whole material. The interlayer separation is in fact too small to accommodate large molecules, but a standard procedure employs intercalation in two steps: firstly small molecules (for example ethanol) and subsequently larger ones. In particular, it has been shown [20] that the intercalation of large molecules such as polyamines can be used to exfoliate ZP. Our data in Fig. 2 clearly are consistent with such a phenomenon occurring upon gel formation with PVA and glycerine. It is reasonable to assume that glycerine intercalation and ensuing exfoliation are most efficient under conditions of slow drying, which accounts for the data in curve (d) of Fig. 2.

The role of the PVA, we believe, is essential for stabilizing the exfoliated ZP fragments in the glycerine. Figure 3 gives a schematic representation of the path for preparing the ZP/PVA/glycerine composite electrolyte. Further support for this model was gained from thermal analysis data, as discussed next.

Thermal analysis by DSC

The thermal properties of the samples were analysed using a Mettler-Toledo DSC 30 instrument with a Mettler TC 10A/TC15 system control unit. The studies were performed in the $-130\ °C < T < 180\ °C$ temperature range, with heating in a nitrogen flux at a rate up to 5 K/min, and cooling at 100 K/min. Figure 4 shows the DSC results for ZP powders dried under different conditions, with the exothermic heat flow pointing upwards. Two endothermic features (minima) occur for $Zr(HPO_4)_2{\cdot}3.7H_2O$, as apparent from curve (a). The first broad minimum at 100 °C is connected with adsorbed water, while the smaller and sharper endothermic minimum at 150 °C is probably related to a loss of water from the layers so that the powder is irreversibly changed. This interpretation is supported by the observation that the minimum assigned to water adsorption in curve (a) disappears after heat treatment of the sample at 105 °C in a dry nitrogen flow, while the sharp peak at 150 °C remains unchanged (cf. curve b in Fig. 4), and by the disappearance of the endothermic DSC minimum at 150 °C upon annealing at 160 °C or on vacuum treatment (cf. curves c and d in Fig. 4). After equilibrating

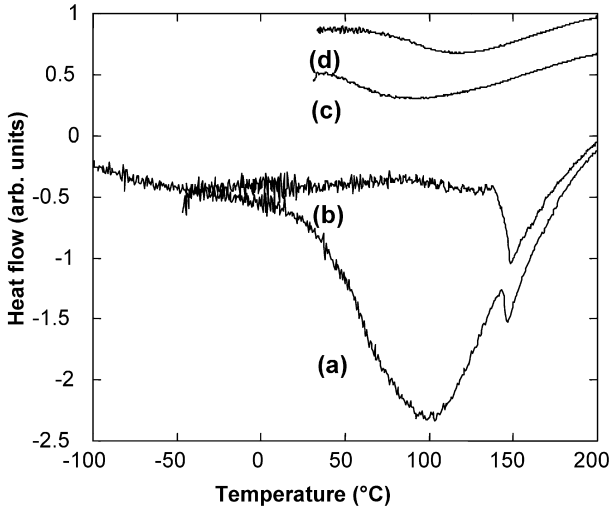

Fig. 4 DSC data for (*a*) $Zr(HPO_4)_2{\cdot}3.7H_2O$, (*b*) the sample dried at 105 °C, (*d*) after drying the sample under vacuum, and (*c*) for $Zr(HPO_4)_2{\cdot}2.9H_2O$. Minima correspond to endothermic features

the samples treated at 105 °C under room conditions, it was possible to regain the DSC features characteristic for $Zr(HPO_4)_2{\cdot}3.7H_2O$. The rise of the baseline of curves (a) and (b) on the high temperature side, as shown in Fig. 4, is probably due to the decrease of the sample mass after evaporation of water.

Figure 5 shows DSC data for two ZP/PVA/glycerine materials, as well as for pure glycerine. Materials containing 18–24 wt% ZP, which displayed maximum proton conductivity and visual transparency, as discussed below, have an endothermic feature with an onset at 134 °C, which is evident from curve (a) in Fig. 5. Materials with a ZP content lower than 18 wt% and larger than 24 wt%, on the other hand, have broad endothermic features centered at 130 °C (cf. curve b in Fig. 5). We believe that these latter samples contain weakly bonded water whose removal accounts for the smooth variation of the DSC curve from room temperature onwards. On the other hand, pure glycerine shows a flat response in the same temperature region (cf. curve c in Fig. 5). The feature at ~ -83 °C for pure glycerine (curve c) is an indication of the glass transition temperature, T_g, of supercooled glycerine. In the samples containing PVA and ZP, the glass transition is found to be decreased to −96 °C. This unambiguous shift is taken as evidence for a thorough dispersion of

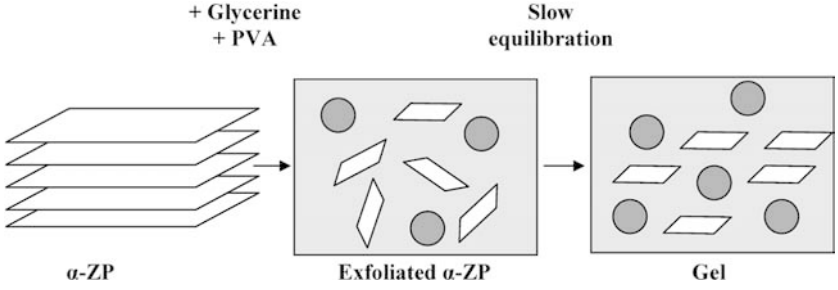

Fig. 3 Schematic representation of the formation of ZP/PVA/glycerine electrolytes incorporating exfoliated ZP fragments. The *dark circles* indicate PVA particles

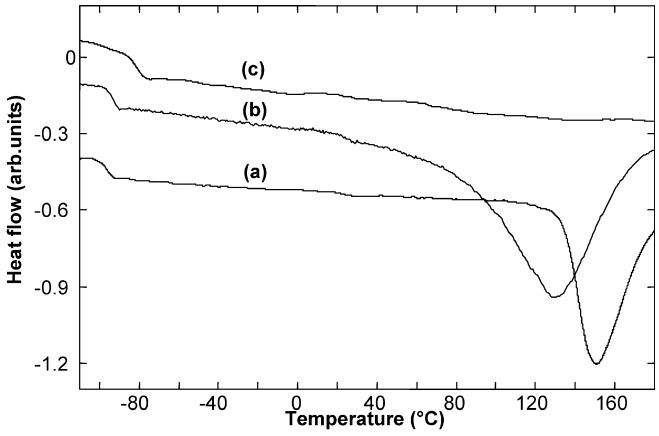

Fig. 5 DSC data for ZP-based gels with ZP contents of (*a*) 24 wt% and (*b*) 30 wt%, and (*c*) for pure glycerine

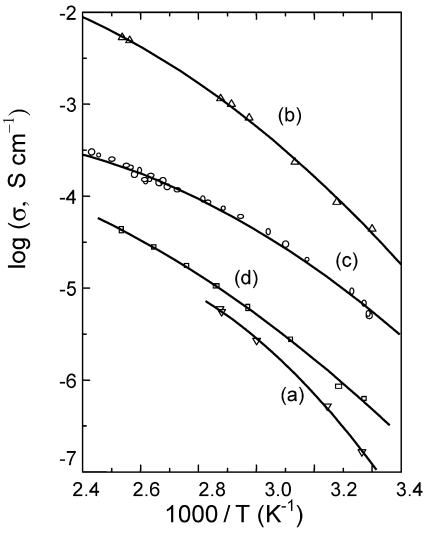

Fig. 6 Temperature dependence of the conductivity σ for ZP/PVA/glycerine gel electrolytes with a ZP content of (*a*) 10 wt%, (*b*) 18 wt% (b), (c) 24 wt%, and (*d*) 32 wt% at a relative humidity below 1%. Data are shown at temperatures between 20 °C and 130 °C. *Symbols* denote measured data points and *curves* were obtained from the VTF equation (Eq. 1) using the parameter values in Table 1

the glycerine and a reduced interaction in these materials of the OH groups, characteristic of pure glycerine.

Electrical and optical data

Conductivity by impedance spectroscopy

Impedance spectroscopy was applied to the ZP/PVA/glycerine materials by use of a Solartron 1260 Frequency Response Analyser. Data were taken from lower to higher temperatures in the 20 °C < T < 130 °C range, and conductivities were evaluated from plots of complex resistivity. The samples were equilibrated in differently humidified atmospheres, specifically with a relative humidity of 100, 31, and < 1%.

Table 1 summarizes data on the conductivity, σ. Measurements of σ for 20 °C < T < 130 °C showed non-linearity when plotted in the conventional Arrhenius coordinates (Fig. 6). However, the temperature variation could be well described within the framework of the Vogel–Tamman–Fulcher (VTF) empirical equation [21], which states that:

$$\sigma(T) = AT^{-1/2}\exp[-B/k_B(T - T_0)] \quad (1)$$

where T_0 is an equilibrium glass transition temperature, A is a pre-exponential factor, B is a pseudo-activation energy for conduction, and k_B is Boltzmann's constant.

The VTF equation is commonly employed for describing ion conductivity of amorphous polymers [22] and amorphous regions of mixed phase materials. In the present study, T_0, ln(A), and B were found to depend on the amount of ZP in the electrolyte. Composites with ZP contents outside the 18–24 wt% range contain weakly bonded adsorbed water which is lost during heating, as seen in curve (a) of Fig. 5. The water loss increased the curvature of the σ vs. T dependence in an Arrhenius diagram. In this compositional interval the evaluated T_0 values were lower than T_g. The curvature of the σ vs. $1/T$ relationship can be accounted for by the VTF equation, as shown by the correlation coefficient, R^2. The values of ln(A) and B display a maximum for a ZP concentration equal to 18 wt% and in general a reciprocal linear correlation, which according to the Meyer–Neldel rule [23] suggests a dependence of the conduction on the ion mobility more than on the density of the charge carriers.

Both major ingredients of the studied electrolyte – the ZP powder and the PVA/glycerine gel – are highly

Table 1 Equilibrium glass transition temperature T_0, glass transition temperature T_g, correlation coefficients for the Arrhenius and VTF equations, VTF equation parameters [ln(A), B], and electrical conductivity for ZP/PVA/glycerine gels with different amounts of ZP. Before the conductivity measurements the composites were treated for 24 h at 298 K in environments with different relative humidities (RH). The correlation coefficients R^2 were calculated with a least-squares routine

ZP content (wt%)	T_0(°C)	T_g(°C)	Correlation coefficient, R^2		ln(A)	B (eV)	log(conductivity in S/cm), at 298 K		
			Arrhenius equation	VTF equation			RH = 100%	RH = 31%	RH < 1%
4.2	–	−96.0	–	–	–	–	−4.3	−7.1	−7.5
10	−58.5	–	0.997	0.9997	0.18	0.66	−3.5	−5.5	−6.7
18	−100.5	−96.1	0.993	0.999	3.3	1.14	−2.6	−4.0	−4.4
24	−97.6	−96.1	0.989	0.997	1.1	0.81	−3.6	−4.3	−5.2
32	−62.5	−91.5	0.996	0.997	0.15	0.60	−3.9	−5.3	−6.3

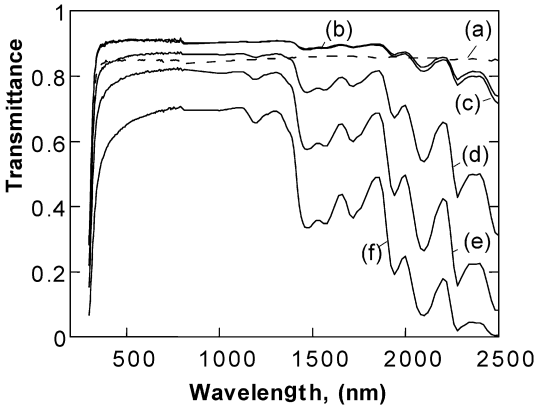

Fig. 7 Spectral transmittance of ZP/PVA/glycerine electrolytes with thicknesses of (*b*) 0.04 mm, (*c*) 0.07 mm, (*d*) 0.20 mm, (*e*) 0.45 mm, and (*f*) 0.93 mm. The electrolyte layers were pressed between two glass substrates. The dashed curve (*a*) refers to a bare glass substrate

hygroscopic. Both are good ion conductors at high levels of adsorbed water. They lose water upon heating above 60 °C, which causes a decrease of the conductivity by two orders of magnitude, and cooling down does not increase the conductivity again unless fresh water is adsorbed. When the ingredients are mixed to form the electrolyte, the conductivity increases with increasing temperature, and the same path is followed upon heating and cooling, suggesting that the water content in the electrolyte has not decreased upon heating. Apparently, water is more strongly bound in the composite electrolyte than in the separate ingredients. The gels with ZP contents between 18 wt% and 24 wt% showed lower hygroscopicity, and were much more stable to dehydration, than the gels outside this composition range. For these materials in the region 18–24 wt% we also found that T_g is close to T_0 and that σ displayed a maximum.

Transmittance by spectrophotometry

Spectral normal transmittance was recorded in the 250 nm $< \lambda <$ 2500 nm wavelength range, using a Perkin-Elmer Lambda 9 double-beam spectrophotometer, for samples of different thickness. Figure 7 shows that the optical transparency is high in the 400 nm $< \lambda <$ 1200 nm interval, while minima signify pronounced infrared absorption at longer wavelengths. The visual transparency indicates that the ZP particles are small enough to be essentially non-scattering for luminous radiation. Specifically, the transmittance at 550 nm is 0.91 for a 40-μm-thick layer. A small particle size also tends to yield a large electrical conductivity, as reported in the literature [24].

Conclusions

This work has described the synthesis of a new proton-conducting gel electrolyte composed of zirconium phosphate, PVA, and glycerine. A combination of measurements demonstrated electrical, optical, and thermal properties that render this material suitable for electrochromic devices. Exfoliation of zirconium phosphate due to intercalation of glycerine seems to be the mechanism underlying the dispersion of the nanoparticles in the PVA/glycerine gel.

References

1. Granqvist CG (1995) Handbook of inorganic electrochromic materials. Elsevier, Amsterdam
2. Granqvist CG (1999) Electrochim Acta 44:3005
3. Granqvist CG (2000) Solar Energy Mater Solar Cells 60:201
4. Slade RCT, Knowles JA, Jones DJ, Roziere J (1997) Solid State Ionics 96:9
5. Vaivars G, Azens A, Granqvist CG (1999) Solid State Ionics 119:269
6. Yang C, Srinivasan S, Aricò AS, Cretì P, Baglio V, Antonucci V (2001) Electrochem Solid-State Lett 4:A31
7. Costamagna P, Yang C, Bocarsly AB, Srinivasan S (2002) Electrochim Acta 47:1023
8. Jones DJ, Roziere J (2001) J Membr Sci 185:41
9. Alberti G, Casciola M, Palombari R (2000) J Membr Sci 172:233
10. Bonnet B, Jones DJ, Roziere J, Tchicaya L, Alberti G, Casciola M, Massinelli L, Bauer D, Peraio A, Ramunni E (2000) J New Mater Electrochem Syst 3:87
11. Honma I, Nomura S, Nakajima H (2001) J Membr Sci 185:83
12. Clearfield A, Stynes JA (1964) J Inorg Nucl Chem 26:117
13. Alberti G, Toracca B (1968) J Inorg Nucl Chem 30:317
14. Dushin R, Krylov V (1978) Izv Akad Nauk SSSR Neorg Mat 14:288
15. Clearfield A, Troup JM (1977) Inorg Chem 16:3311
16. Schuck G, Melzer R, Sonntag R, Lechner RE, Bohn A, Langer K, Casciola M (1995) Solid State Ionics 77:55
17. Costantino U, Vivani R, Zima V, Cernoskova E (1997) J Solid State Chem 132:17
18. Casciola M, Costantino U, Marmottini F (1989) Solid State Ionics 35:67
19. Costantino U, Casciola M, Pani G, Jones DJ, Roziere J (1997) Solid State Ionics 97:261
20. Glipa X, Leloup JM, Jones DJ, Roziere J (1997) Solid State Ionics 97:227
21. MacCallum JR, Vincent CA (eds) (1987) Polymer electrolyte reviews, vol 1. Elsevier Applied Science, London
22. Albinsson I, Mellander B-E, Stevens JR (1992) J Chem Phys 96:681
23. Goldie DM (2001) Defect Diffus Forum 192–193:27
24. Krogh Andersen E, Krogh Andersen IG, Knakkergard Moller C, Simonsen KE, Skou E (1982) Solid State Ionics 7:301